Modelling of resonances in the $\gamma p \to \eta \pi^0 p$ reaction

Author: Elisabeth Llanos Pla

Facultat de Física, Universitat de Barcelona, Diagonal 645, 08028 Barcelona, Spain.

Advisor: Vincent Mathieu

Abstract: High-energy reactions produce short-lifetime intermediate states —resonances— which can only be studied by analyzing the properties of the resulting particles of their decay. Some mesonic resonances do not correspond to a normal $q\bar{q}$ system since their quantum numbers are forbidden by the current quark model, giving rise to exotic mesons. In this work, we build a model to recreate the $\gamma p \to \eta \pi^0 p$ high-energy reaction in which an exotic meson is produced, and we include baryonic resonances to study their impact on the mesons interaction $\eta \pi^0$. Our results point out that the relative contribution of baryons decreases as the photon's energy increases.

I. INTRODUCTION

The study of exotic-quantum-number mesons is increasingly gaining ground within the Nuclear Physics community. These mesons, also known as exotic mesons or hybrid mesons, consist of a quark and an anti-quark ($q\bar{q}$) bounded by an excited gluonic field constituting a system whose quantum numbers J^{PC} are not allowed by the current quark model [1]. To obtain these subatomic particles, high-energy reactions such as $\gamma p \to \eta \pi^0 p$ are required. The aforementioned scattering consists of a fixed energy photon that collides with a proton, resulting in a three-particle final state, whose constituents can be considered stable. Nonetheless, high energy reactions have proven the existence of additional short-lifetime states which decay through the strong interaction, giving rise to the detected final particles. These intermediate states are known as resonances, and some of them could be exotic mesons. Due to their brief presence, it is only possible to witness their existence by analyzing the final particles in which they decay.

Previous research [2, 3] have confirmed the existence of hybrid mesons such as $J^{PC} = 1^{-+}$ (named after $\pi_1(1600)$). Other exotic mesons have been detected, and new predictions have been made by the Quantum Chromodynamics (QCD) theory and the Flux Tube model [4]. These predictions, if confirmed by the subsequent detection, may suggest that the current quark model should be revised.

In this paper, we take as reference the GlueX photoproduction experiment at Jefferson Lab [5], whose aim is to search for hybrid mesons with masses up to 2 GeV/c^2. In a recent preliminary project [2], a large amount of data has been collected on the production of particles resulting from different decayed resonances of the $\gamma p \to \eta \pi^0 p$ reaction. The results of the several experiments have been gathered and displayed in a so-called "COMPASS plot", presented for the first time by the COMPASS collaboration [6]. The latter is a two-dimensional scatter plot of the events' distribution of the reaction under consideration; therefore, it is an optimal technique to visualize the existence of resonances and their probability.

In the aforementioned reaction, each possible couple of final particles define a channel (ij $\equiv \eta \pi^0, \eta p, \pi^0 p$). Its main interest lies in the analysis of the resonances in the two final mesons channel $\eta \pi^0$, since one of the plausible resonances corresponds to an exotic state: π_1. The main constraint one is inevitably forced to face is the presence of resonances in other channels (ηp and $\pi^0 p$), which overlap with the exotic state in the COMPASS plot, hindering its proper study. A standard experimental procedure to deal with cross-channel resonances, *i.e.* baryons in our case, is simply to remove them by appropriate mass cuts (for more information see [2]). In spite of this, part of the angular distribution with regard to the $\eta \pi^0$ resonances is lost. The reaction should be studied as a whole; it is not a rigorous strategy to wipe out part of the information. This is the reason why there is a growing need to simulate these reactions and create models, which has been the motivation of our work.

In our work, we focus on the $\gamma p \to \eta \pi^0 p$ reaction as well, in order to compare our results with those obtained by the GlueX preliminary project. The purpose of our work is to build a model to recreate the reaction in a COMPASS plot, so as to ease the understanding of the separate resonances. Furthermore, our ambition is to come upon a solution to reduce the presence of the resonances in the ηp and $\pi^0 p$ channels, in order to enable the accurate study of the exotic meson without removing information. The results point out that an increase in the incident photon's energy would lessen the presence of baryonic resonances.

The rest of the paper is organized as follows: in section II we provide a brief overview of the theoretical framework, in section III we go into detail on the formulation of our model, in section IV we display the resulting COMPASS plots, and in section V we conclude the paper.

II. THEORETICAL FRAMEWORK

A. Quantum Numbers

Quantum numbers of a 2-particle system, such as the couple's relative angular momentum (L), its projection on z-axis ($-L \leq m \leq L$), spin (S), total spin (J), parity

(P) or C-parity (C), are discrete numbers linked to specific variables describing the various states of a system. These quantum numbers cannot take arbitrary values, but are correlated in compliance with the rules:

$$\vec{J} = \vec{L} + \vec{S} \implies |L - S| \leq J \leq L + S \qquad (1)$$

$$P = P_1 P_2 (-1)^L \qquad C = (-1)^{L+S} \qquad (2)$$

Where $P_1, P_2 = \pm 1$ is the intrinsic parity of a particle composing the system. These rules also apply to a $q\bar{q}$ couple, taking into account that $P_q = -P_{\bar{q}}$, forbidding certain quantum numbers combinations [1]. One can check that some of the possible quantum numbers combinations are the following: $J^{PC} = 0^{++}, 2^{++}, 1^{--}$, but others such as 1^{-+} are not allowed.

π_1 is one of the resonances we deal with, decaying to η and π^0. It has $J^{PC} = 1^{-+}$. Therefore, this resonance cannot be constituted by a quark and an antiquark; we find ourselves facing an exotic meson.

B. Kinematics: Scattering of two particles into three particles

It is known that the π_1 resonance can be produced in the following reaction:

$$\gamma p \to \eta \pi^0 p$$

In which the resulting proton has, in general, a different energy and direction in comparison to its initial state.

The derivation of the kinematics involved in such high-energy reactions can be far from trivial, since several variables and scattering angles are implicated. However, not all of them are independent. A set of N particles moving without restraint has $3N$ levels of freedom, but taking into account the 10 symmetries of the Poincaré Group (3 rotations, 3 translations and 4 boosts) the number of degrees of freedom, k, needs to be recalculated as follows: $k = 3N - 10$. In our particular case, $N = 5$ and consequently $k = 5$, pointing out that the whole kinematics of the reaction can be described using five variables.

On the other hand, we are forced to deal with three distinctive reference systems R_{ij}, one for each channel, in which the sum of the momenta of the resulting particles i, j equals zero. Since a resonance's spin is defined in the rest frame of the corresponding couple of final particles, it is imperative to characterise the three reference systems, named Gottfried-Jackson (GJ) frames. To mitigate this issue, it is essential to define Lorentz-invariant variables, which take the same value in the distinctive GJ frames. These are known as Mandelstam variables [7], and they relate the four-momentum of a couple of particles in the reaction. We can define them as:
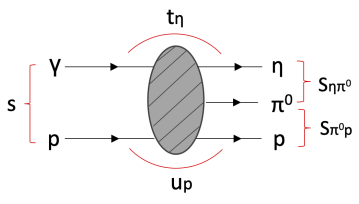
$$s = (P_\gamma^\mu + P_p^\mu)^2$$
$$s_{ij} = (P_i^\mu + P_j^\mu)^2$$
$$t_i = (P_\gamma^\mu - P_i^\mu)^2$$
$$u_i = (P_p^\mu - P_i^\mu)^2$$

$$(3)$$

Figure 1: $\gamma p \to \eta \pi^0 p$ reaction.

The four-momenta are defined within the Minkowski metric as $P_i^\mu = (p_i^0, \vec{p_i}) = (E_i, \vec{p_i})$, using units of c $= 1$. $\vec{p_i}$ is the linear momentum of the particle i, and E_i its energy. These variables cannot take arbitrary values, since conservation of momentum and energy must be fulfilled. In a relativistic approach, these two quantities and the rest mass m_i are related through the following equation:

$$E_i = \sqrt{p_i^2 + m_i^2} \qquad (4)$$

The energy and momentum of each particle can be determined in each frame R_{ij} in terms of the corresponding Mandelstam variable s_{ij}, also referred to as invariant mass. The derivation of those expressions can be done following the procedure detailed in [7], chapter V.

C. Resonances

Resonances are the potential intermediate states from which two of the three particles arise. These resonances are characterised by a scattering amplitude A. The corresponding expression used in our model is given in section III, Eq. (10). The scattering amplitude is a probability amplitude, whose squared modulus is a key magnitude to determine the total differential cross-section of the reaction $d\sigma/d\tilde{\Omega}$, which can be computed within different domains $\tilde{\Omega}$. As explained in section II.B, five variables are needed to describe the entire kinematics of the reaction. To build a COMPASS plot, we conveniently choose to work with the following set of variables:

$$\text{s}, \, s_{\eta\pi^0}, \, u_p, \, \theta_{\eta\pi^0}, \, \phi_{\eta\pi^0}$$

Being $\theta_{\eta\pi^0}$ and $\phi_{\eta\pi^0}$ respectively the polar and azimuth angles of $\vec{p_\eta}$ defined in the $R_{\eta\pi^0}$ reference frame. This definition also encompasses that the photon beam is traced along the z-axis and the resulting proton lives in the x-z plane. Moreover, the variable s, which is referred to the initial photon's energy, is set to a fixed value.

Since our objective is to recreate a COMPASS plot, in which one displays the the total differential cross-section given a specific value of $s_{\eta\pi^0}$ and $cos(\theta_{\eta\pi^0})$, we need to integrate for all the possible values of the other variables we chose. The total differential cross-section in the $s_{\eta\pi^0}$ - $cos(\theta_{\eta\pi^0})$ domain reads as:

$$\frac{d\sigma}{d\sqrt{s_{\eta\pi^0}}d\cos(\theta_{\eta\pi^0})} = \int_0^{2\pi} \int_{u_p^-}^{u_p^+} \frac{389\rho(s_{\eta\pi^0})|A|^2}{(4\pi)^4(s - m_p^2)^2} d\phi_{\eta\pi^0} du_p$$

$$(5)$$

Where $\rho(s_{\eta\pi^0}) = \sqrt{\lambda(s_{\eta\pi^0}, m_\eta^2, m_{\pi^0}^2)}/(2\sqrt{s_{\eta\pi^0}})$ with the λ function defined as:

$$\lambda(a,b,c) = a^2 + b^2 + c^2 - 2(ab + ac + bc) \qquad (6)$$

We added $(\hbar c)^2 = 389$ GeV$^2\mu$b to express the cross section in physical units. Eq. (5) can be derived from the phase space integral definition. u_p^+ and u_p^- are the maximum and minimum values of the invariant u_p (for detailed procedure see [7], chapter V):

$$u_p^\pm = 2m_p^2 - \frac{1}{2s}[(s + m_p^2)(s - s_{\eta\pi^0} + m_p^2)$$
$$\mp \lambda^{1/2}(s, 0, m_p^2)\lambda^{1/2}(s, s_{\eta\pi^0}, m_p^2)] \qquad (7)$$

III. MODEL DEVELOPMENT

Once we understand the complex kinematics involved in the reaction and the possible resonant states, we are ready to proceed to re-create the results obtained by the GlueX experiment (see Figure 4). To do so, we develop a simple and rather faithful Python-model of the $\gamma p \rightarrow \eta\pi^0 p$ reaction for a fixed-energy photon of $E_\gamma = 8.5$ GeV in the laboratory frame; as in the GlueX experiment. Applying the kinematics equations and the cross-section formulas, we can generate the dominant resonances for each channel in a COMPASS plot for the subsequent analysis of these states. In a COMPASS plot, $s_{\eta\pi^0}$ and $cos(\theta_{\eta\pi^0})$ are the variables that we respectively display on the x and y axis. The region in which the events are represented is delimited by the possible values of the invariant mass $s_{\eta\pi^0}$, which are constrained by the initial energy E_γ. Only events within this region are physically allowed.

In the first place, we assume scalar particles, meaning they have a spin equal to zero and they remain invariant under Lorentz transformations. With this approximation, we are presuming a non-polarized photon and nucleons.

To create such a model we follow the procedure:

1. Firstly, we fix the energy of the photon to $E_\gamma = 8.5$ GeV. We also determine the invariant mass s, which expanding the first expression of Eq. (3) reads as:

$$s = m_\gamma^2 + m_p^2 + 2E_\gamma E_p - 2\vec{p}_\gamma \cdot \vec{p}_p = m_p^2 + 2m_p E_\gamma \quad (8)$$

2. We determine the COMPASS plot boundaries, that is, the possible $s_{\eta\pi^0}$ domain. Expanding $s_{\eta\pi^0}$ similarly to the previous step, one can grasp that its minimum value can be mathematically computed by maximizing the product of the concerning 4-momenta and enforcing a border case. Straightaway, it can easily be noticed that $s_{\eta\pi^0(min)}$ is obtained when both resulting particles η and π^0 are at rest, and the final p inevitably acquires the total momentum given its conservation. By analogy, when this proton is at rest and the momentums of η and π^0 take an equal and highest value, the maximum

permitted $\eta\pi^0$ invariant mass is reached. Taking these assertions into account and making use of Eq. (4), the physical $s_{\eta\pi^0}$ allowed region can be determined:

$$(m_\eta + m_{\pi^0})^2 < s_{\eta\pi^0} < (\sqrt{s} - m_p)^2 \qquad (9)$$

On the other hand, $-1 < \cos(\theta_{\eta\pi^0}) < 1$. Once the plot boundaries have been set, given a fixed step we discretize the inside of this effective region.

3. The next step is to define the intermediate states. The most likely resonances for each channel have been included in our model (represented in Figure 2), whose characteristic parameters, appearing in Eq. (10), can be found in Table I.
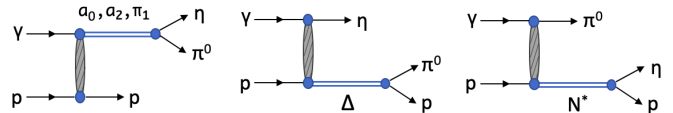

Figure 2: Included resonances for each production channel.

The total scattering amplitude of the reaction for the included resonances can be expressed by means of a partial wave expansion:

$$A = \sum_{ij, i<j} A_{ij} = \sum_{ij, i<j} \sum_R (2L_R + 1)f_{L_R}(s_{ij})Y_{L_R m}(\phi_{ij}, \theta_{ij})$$
$$= \sum_{ij, i<j} \sum_R (2L_R + 1)\left[\frac{-a \cdot s^{0.9k_{ij}+0.5}}{s_{ij} - M^2 + i\Gamma\sqrt{s_{ij}}}\right]Y_{L_R m}(\phi_{ij}, \theta_{ij})$$
$$(10)$$

In Eq. (10) we sum the contribution of all the resonances, R, in each channel ij. L_R denotes the angular momentum of the resulting particles of the decayed resonance, $f_{L_R}(s_{ij})$ the partial amplitude depending on the invariant mass of each channel, and $Y_{L_R m}(\phi_{ij}, \theta_{ij})$ the spherical harmonic functions. We have expressed the partial amplitude as a constant-width Breit-Wigner (BW) function [8], where M is the total mass of the resonance, i the imaginary unit, and Γ the width of the resonance. The latter is related to the mean lifetime of the state in the non-relativistic limit, τ, according to $\Gamma = 1/\tau$. The constant-width Breit-Wigner parameterization is a continuous probability distribution, and it is accurate to characterize narrow and isolated resonances of scalar particles. Its poles' positions determine the energy of the resonances, since its expression is derived from considering the wave function of a decaying state. Moreover, the BW formula includes a term, $a \cdot s^{0.9k_{ij}+0.5} \equiv a \cdot s^{\alpha(k_{ij})}$, referred to the coupling of the intermediate state to the initial and final states, with $k = u_p, t_\eta, t_{\pi^0}$ for $ij = \eta\pi^0, \eta p, \pi^0 p$ respectively. To calculate the amplitude of each resonance, energies and angles have to be computed for each reference frame. To do so, we work out the kinematics equations involved in the reaction and we use the relations between Mandelstam invariants found in [7], chapter V.

Table I: Angular momentum (L), its projection on z axis (m), mass (M), width (Γ) and branching ratio (a) for each of the resonances included in our model.

Resonance	Channel	J^{PC}	L	m	M(GeV)	Γ(GeV)	a
$a_0(980)$	$\eta\pi^0$	0^{++}	0	0	0.980	0.075	0.725
$\pi_1(1600)$	$\eta\pi^0$	1^{-+}	1	1	1.660	0.241	0.100
$a_2(1320)$	$\eta\pi^0$	2^{++}	2	1	1.318	0.107	0.421
$\Delta(1232)$	$\pi^0 p$	$\frac{3}{2}^+$	1	1	1.231	0.117	0.616
$N^*(1535)$	ηp	$\frac{1}{2}^-$	0	0	1.530	0.150	0.399

Masses, quantum numbers, branching ratios, and widths have been obtained from the Particle Data Group database [9], as well as from [10]. The value of m has been set in compliance with previous studies [6].

4. To make our model more realistic, we introduce a Double Regge term [11] to simulate the events for large $s_{\eta\pi^0}$ values. In this region of the plot, we expect a lack of resonances since the probability of interaction is smaller. We used a rough expression for the amplitude (Eq. (11)), where a_1^{DR} and a_2^{DR} have been set to arbitrary values.

$$A^{DR} \propto a_1^{DR} s_{\eta\pi^0}^{\alpha(t_{\pi^0})} s_{\pi^0 p}^{\alpha(u_p)} + a_2^{DR} s_{\eta\pi^0}^{\alpha(t_\eta)} s_{\eta p}^{\alpha(u_p)} \quad (11)$$

5. The next step is to compute the total cross-section $d\sigma/d\sqrt{s_{\eta\pi^0}}dcos(\theta_{\eta\pi^0})$ of the reaction using Eq. (5). We solve the integral numerically for each $(s_{\eta\pi^0}, cos(\theta_{\eta\pi^0}))$ point in which we discretized the physical region of production. The result of each integration gives an idea of the probability of an event characterized by specific $s_{\eta\pi^0}$ and $cos(\theta_{\eta\pi^0})$. Finally, we make a density plot of the cross-section in which the different resonances reveal.

IV. RESULTS AND ANALYSIS

We have been able to recreate the various events that occurred in a $\gamma p \rightarrow \eta\pi^0 p$ reaction using the model we created. Figure 3 shows the resulting COMPASS plot.

Analysing the plot shown in Figure 3, one can witness the five different included resonances. The vertical thin line on the left corresponds to a_0, which can also be appreciated in the GlueX experiment plot (Figure 4). In the latter, it exhibits as a non-uniform band due to the imperfect acceptance of the detector. Next to a_0, the resonance a_2 is clearly visible in Figure 3 with nodes where the cosine equals -1, 0 and 1, in accordance to its definition. Furthermore, the exotic meson π_1 exhibits as a dizzy vertical band, overlapping with the a_2 resonance. A slight asymmetry can be observed in that region, which arises as a result of the squared modulus of the sum of the cosine and sine appearing on the spherical harmonics of a_2 and π_1 respectively. The intermediate state a_2 can also be seen in Figure 4, but the nodes are not well-defined. The lack of nodes can be attributed to electromagnetic background (e^+e^- pair) and
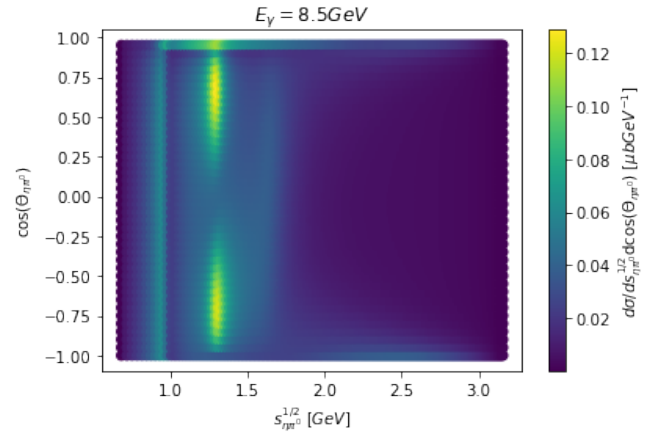

Figure 3: Total differential cross-section in the $\sqrt{s_{\eta\pi^0}}$ - $cos(\theta_{\eta\pi^0})$ domain for a fixed photon energy $E_\gamma = 8.5 GeV$.
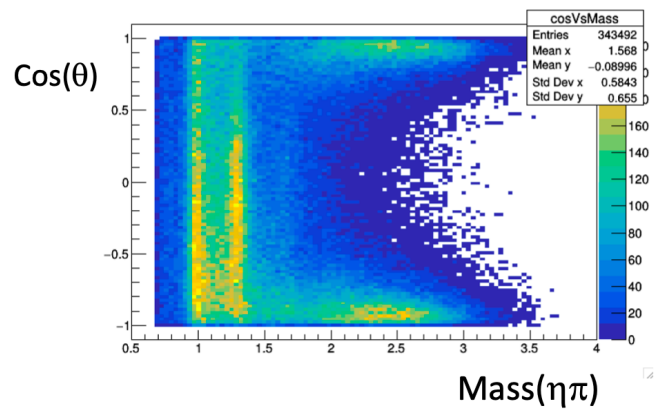

Figure 4: GlueX experiment collected data representing the total differential cross-section in the $\sqrt{s_{\eta\pi^0}}$ - $cos(\theta_{\eta\pi^0})$ domain for a fixed photon energy $E_\gamma = 8.5 GeV$.

unavoidable detector irregularities (for more information see [5]). In addition to this, the exotic meson interferes with a_2, breaking its inherent symmetry. From these results, we can deduce that the asymmetry within the a_2 region is an indicator of the presence of exotics. Nevertheless, the two horizontal bands, which correspond to the baryonic resonances Δ and N^*, disturb the study of hybrids. One can see that they intersect the intermediate meson states, contributing to additional asymmetries that could be wrongly attributed to exotics.

It is important to remark that our model is based on some approximations that also contribute to causing dissimilarities between our plot and GlueX's. As mentioned, we considered scalar particles and only the most common resonances. Nonetheless, these approximations seem to be valid since our results have proven to be consistent.

One of the advantages of our model is that it enables us to study the resonances separately. We have control over the different parameters, which can be adjusted in order to inspect various scenarios and see how our system

behaves. By simulating multiple alternatives, we found that an increase in the initial energy of the photon beam would reduce the baryonic resonances, leading to a mitigation of the effect of those resonances on the mesonic intermediate states. We numerically verified that, in such a situation, the amplitude of both baryonic and mesonic resonances acquires a higher value, but the baryonic ones present a much slower rise in accordance to the increasing energy. Therefore, doubling the photon energy to $E_\gamma = 17 GeV$, we obtained the results shown in Figure 5: a significant reduction of the amplitude of the baryonic resonances (Δ, N^*) in comparison with stronger evidence of the mesonic resonances (a_0, a_2, π_1). Hence, an increase of the E_γ is a more rigorous alternative to study the mesonic resonances (and exotic states) rather than removing the baryonic bands, which would cause a loss of useful mesonic data.
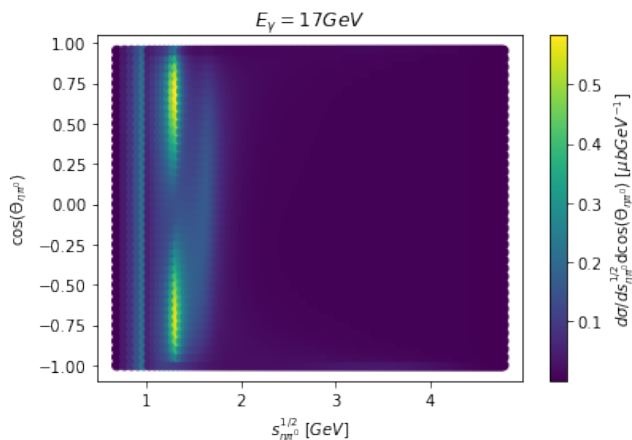

Figure 5: Total differential cross-section in the $\sqrt{s_{\eta\pi^0}}$ - $cos(\theta_{\eta\pi^0})$ domain for a fixed photon energy $E_\gamma = 17$ GeV.

Setting aside the satisfactory results, it is essential to be aware of the positive contribution of such models to the Nuclear Physics community since they help to understand the physics behind the experimental results and enable us to do predictions.

V. CONCLUSIONS

After studying the kinematics involved in a scattering of 2 particles into 3 particles and doing research on the decay of resonances and its quantum numbers, we successfully built a model which re-creates the $\gamma p \to \eta\pi^0 p$ reaction. Using a partial wave expansion and the Breit-Wigner parameterization, we included some of the probable resonances in each decay channel for a fixed energy of the initial photon beam. Those resonances reveal as perceptible bands when plotting the total differential cross-section of the reaction for a fixed value of $\sqrt{s_{\eta\pi^0}}$ and $cos(\theta_{\eta\pi^0})$. The resulting COMPASS plot resembles the one provided by the GlueX experiment, with slight differences in the behaviour of the a_2 meson and the Δ baryon. These discrepancies are attributed to detector restrictions and background altering the expected real results, as well as to idealistic approximations considered in our model. Notwithstanding the foregoing, we have been able to qualitatively represent the resonances and detect the asymmetries caused by the presence of an exotic meson. Moreover, we determined that a rise in the photon's energy lessens the presence of baryonic resonances, smoothing the way for the study of hybrid mesons, which is the objective of the current investigations involving high-energy reactions.

[1] Meyer, Curtis A., and Y. Van Haarlem. "Status of exotic-quantum-number mesons." Physical Review C 82.2 (2010): 025208.

[2] Barsotti, Rebecca. "Double-Regge Physics in $\eta\pi^0$ at the GlueX Experiment." Bulletin of the American Physical Society (2022).

[3] Thompson, D. R., et al. "Evidence for Exotic Meson Production in the Reaction $\pi^- p \to \eta\pi^- p$ at 18 GeV/c." Physical Review Letters 79.9 (1997): 1630.

[4] Ketzer, Bernhard. "Hybrid mesons." arXiv preprint arXiv:1208.5125 (2012).

[5] J. Pinfold, D. Fassouliotis, P. Ioannou, Ch. Kourkoumelis, C. A. Meyer, and The GlueX Collaboration. "The GlueX Experiment: A Search for QCD Exotics Using a Beam of Photons". doc-346 (2004)

[6] Adolph, C., et al. "Odd and even partial waves of $\eta\pi^-$ and $\eta'\pi^-$ in $\pi^- p \to \eta'\pi^- p$ at 191 GeV/c." Physics Letters B 740 (2015): 303-311.

[7] E. Byckling, K.Kajantie. *Particle Kinematics*, (John-Wiley Sons, Helsinki 1972)

[8] P. A. Zyla *et al.* [Particle Data Group], "Review of Particle Physics," PTEP (2020) no.8, 083C01

[9] Particle Data Group webpage: https://pdg.lbl.gov/

[10] Mathieu, V., et al. "Exclusive tensor meson photoproduction." Physical Review D 102.1 (2020): 014003.

[11] Shimada, T., Alan D. Martin, and A. C. Irving. "Double Regge exchange phenomenology." Nuclear Physics B 142.3 (1978): 344-364.